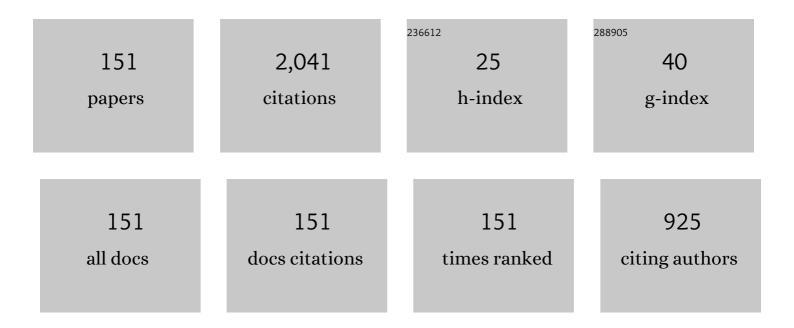


List of Publications by Year in descending order

Source: https://exaly.com/author-pdf/8928439/publications.pdf Version: 2024-02-01



7HANC

#	Article	IF	CITATIONS
1	A review on image reconstruction algorithms for electrical capacitance/resistance tomography. Sensor Review, 2016, 36, 429-445.	1.0	155
2	Development of a fan-beam TDLAS-based tomographic sensor for rapid imaging of temperature and gas concentration. Optics Express, 2015, 23, 22494.	1.7	104
3	An image reconstruction algorithm based on total variation with adaptive mesh refinement for ECT. Flow Measurement and Instrumentation, 2007, 18, 262-267.	1.0	93
4	Online Cross-Sectional Monitoring of a Swirling Flame Using TDLAS Tomography. IEEE Transactions on Instrumentation and Measurement, 2018, 67, 1338-1348.	2.4	79
5	Reconstruction of Axisymmetric Temperature and Gas Concentration Distributions by Combining Fan-Beam TDLAS With Onion-Peeling Deconvolution. IEEE Transactions on Instrumentation and Measurement, 2014, 63, 3067-3075.	2.4	68
6	Performance analysis of a digital capacitance measuring circuit. Review of Scientific Instruments, 2015, 86, 054703.	0.6	62
7	Electrical Capacitance Tomography for Sensors of Square Cross Sections Using Calderon's Method. IEEE Transactions on Instrumentation and Measurement, 2011, 60, 900-907.	2.4	56
8	Measurement of nonuniform temperature and concentration distributions by combining line-of-sight tunable diode laser absorption spectroscopy with regularization methods. Applied Optics, 2013, 52, 4827.	0.9	56
9	Frequency-Division Multiplexing and Main Peak Scanning WMS Method for TDLAS Tomography in Flame Monitoring. IEEE Transactions on Instrumentation and Measurement, 2020, 69, 9087-9096.	2.4	56
10	Image reconstruction technique of electrical capacitance tomography for low-contrast dielectrics using Calderon's method. Measurement Science and Technology, 2009, 20, 104027.	1.4	46
11	A High-Speed Digital Electrical Capacitance Tomography System Combining Digital Recursive Demodulation and Parallel Capacitance Measurement. IEEE Sensors Journal, 2017, 17, 6690-6698.	2.4	46
12	Bound states of solitons in a harmonic graphene-mode-locked fiber laser. Photonics Research, 2019, 7, 116.	3.4	41
13	Electrical capacitance tomography with a non-circular sensor using the dbar method. Measurement Science and Technology, 2010, 21, 015502.	1.4	38
14	A Digital Switching Demodulator for Electrical Capacitance Tomography. IEEE Transactions on Instrumentation and Measurement, 2013, 62, 1025-1033.	2.4	38
15	Resolution-doubled one-dimensional wavelength modulation spectroscopy tomography for flame flatness validation of a flat-flame burner. Applied Physics B: Lasers and Optics, 2015, 120, 407-416.	1.1	36
16	Tunable diode laser absorption spectroscopy-based tomography system for on-line monitoring of two-dimensional distributions of temperature and H2O mole fraction. Review of Scientific Instruments, 2016, 87, 013101.	0.6	35
17	Ion current sensing-based lean blowout detection for a pulse combustor. Combustion and Flame, 2017, 176, 263-271.	2.8	34
18	A WMS Based TDLAS Tomographic System for Distribution Retrievals of Both Gas Concentration and Temperature in Dynamic Flames. IEEE Sensors Journal, 2020, 20, 4179-4188.	2.4	31

#	Article	IF	CITATIONS
19	Electrical impedance tomography with an optimized calculable square sensor. Review of Scientific Instruments, 2008, 79, 103710.	0.6	30
20	Relative Entropy Regularized TDLAS Tomography for Robust Temperature Imaging. IEEE Transactions on Instrumentation and Measurement, 2021, 70, 1-9.	2.4	30
21	A calculable sensor for electrical impedance tomography. Sensors and Actuators A: Physical, 2007, 140, 156-161.	2.0	27
22	Flame monitoring of a model swirl injector using 1D tunable diode laser absorption spectroscopy tomography. Measurement Science and Technology, 2017, 28, 054002.	1.4	27
23	Dual-Modality Electrical Tomography for Flame Monitoring. IEEE Sensors Journal, 2018, 18, 8847-8854.	2.4	27
24	A high-speed electrical impedance measurement circuit based on information-filtering demodulation. Measurement Science and Technology, 2014, 25, 075010.	1.4	26
25	Identification of Oil–Water Flow Patterns in a Vertical Well Using a Dual-Ring Conductance Probe Array. IEEE Transactions on Instrumentation and Measurement, 2016, 65, 1249-1258.	2.4	25
26	Direct Image Reconstruction for Electrical Capacitance Tomography Using Shortcut D-Bar Method. IEEE Transactions on Instrumentation and Measurement, 2019, 68, 483-492.	2.4	24
27	A Compact Laser Absorption Spectroscopy Tomographic System With Short Spectral Scanning Time and Adjustable Frame Rate. IEEE Transactions on Instrumentation and Measurement, 2020, 69, 8226-8237.	2.4	24
28	Normalized least-square method for water hold-up measurement in stratified oil–water flow. Flow Measurement and Instrumentation, 2012, 27, 71-80.	1.0	23
29	Reconstruction of two-dimensional velocity distribution in scramjet by laser absorption spectroscopy tomography. Applied Optics, 2019, 58, 205.	0.9	23
30	Four-Terminal Imaging Using a Two-Terminal Electrical Impedance Tomography System. IEEE Transactions on Instrumentation and Measurement, 2014, 63, 432-440.	2.4	22
31	Estimation of Combustion Temperature Field From the Electrical Admittivity Distribution Obtained by Electrical Tomography. IEEE Transactions on Instrumentation and Measurement, 2020, 69, 6271-6280.	2.4	22
32	Multiple parameters× ³ estimation in horizontal well logging using a conductance-probe array. Flow Measurement and Instrumentation, 2014, 40, 192-198.	1.0	21
33	Digital Recursive Demodulator Based on Kalman Filter. IEEE Transactions on Instrumentation and Measurement, 2017, 66, 3138-3147.	2.4	21
34	Direct Image Reconstruction for 3-D Electrical Resistance Tomography by Using the Factorization Method and Electrodes on a Single Plane. IEEE Transactions on Instrumentation and Measurement, 2013, 62, 999-1007.	2.4	19
35	A recursive least squares-based demodulator for electrical tomography. Review of Scientific Instruments, 2013, 84, 044704.	0.6	19
36	Integral inversion to Fraunhofer diffraction for particle sizing. Applied Optics, 2009, 48, 4842.	2.1	18

#	Article	IF	CITATIONS
37	Direct image reconstruction for electrical capacitance tomography by using the enclosure method. Measurement Science and Technology, 2011, 22, 104001.	1.4	18
38	Direct recovery of the electrical admittivities in 2D electrical tomography by using Calderon's method and two-terminal/electrode excitation strategies. Measurement Science and Technology, 2013, 24, 074007.	1.4	18
39	Coil shape optimization of the electromagnetic flowmeter for different flow profiles. Flow Measurement and Instrumentation, 2014, 40, 256-262.	1.0	18
40	lterative Reconstruction Algorithm for Electrical Capacitance Tomography Based on Calderon's Method. IEEE Sensors Journal, 2018, 18, 8450-8462.	2.4	18
41	\$ell_{1}\$-Norm-Based Reconstruction Algorithm for Particle Sizing. IEEE Transactions on Instrumentation and Measurement, 2012, 61, 1395-1404.	2.4	17
42	Real-Time Imaging and Holdup Measurement of Carbon Dioxide Under CCS Conditions Using Electrical Capacitance Tomography. IEEE Sensors Journal, 2018, 18, 7551-7559.	2.4	17
43	A complex programmable logic device-based high-precision electrical capacitance tomography system. Measurement Science and Technology, 2013, 24, 074006.	1.4	16
44	An Agile Electrical Capacitance Tomography System With Improved Frame Rates. IEEE Sensors Journal, 2019, 19, 1416-1425.	2.4	16
45	A Reconfigurable Parallel Data Acquisition System for Tunable Diode Laser Absorption Spectroscopy Tomography. IEEE Sensors Journal, 2017, 17, 8215-8223.	2.4	15
46	Lean blowout detection for bluff-body stabilized flame. Fuel, 2020, 266, 117008.	3.4	15
47	An FPGA-Based On-Chip Neural Network for TDLAS Tomography in Dynamic Flames. IEEE Transactions on Instrumentation and Measurement, 2021, 70, 1-11.	2.4	15
48	Modified Landweber algorithm for robust particle sizing by using Fraunhofer diffraction. Applied Optics, 2014, 53, 6185.	0.9	14
49	Digital signal processor-based high-precision on-line Voigt lineshape fitting for direct absorption spectroscopy. Review of Scientific Instruments, 2014, 85, 123108.	0.6	14
50	Real-Time 3-D Imaging and Velocity Measurement of Two-Phase Flow Using a Twin-Plane ECT Sensor. IEEE Transactions on Instrumentation and Measurement, 2021, 70, 1-10.	2.4	14
51	2D image reconstruction of a human chest by using Calderon's method and the adjacent current pattern. Journal of Instrumentation, 2013, 8, P03004-P03004.	0.5	13
52	Prediction of equivalence ratio in pulse combustor from ion current amplitude spectrum. Fuel, 2018, 218, 179-187.	3.4	13
53	FPGA-Based Real-Time Implementation of Temperature Measurement via Tunable Diode Laser Absorption Spectroscopy. IEEE Sensors Journal, 2018, 18, 2751-2758.	2.4	12
54	Signal Demodulation Methods for Electrical Tomography: A Review. IEEE Sensors Journal, 2019, 19, 9026-9035.	2.4	12

#	Article	IF	CITATIONS
55	Image Reconstruction for Invasive ERT in Vertical Oil Well Logging. Chinese Journal of Chemical Engineering, 2012, 20, 319-328.	1.7	11
56	Noise Immune TDLAS Temperature Measurement Through Spectrum Shifting by Using a Mach–Zehnder Interferometer. IEEE Transactions on Instrumentation and Measurement, 2021, 70, 1-9.	2.4	9
57	A Fuzzy PID-Controlled Iterative Calderon's Method for Binary Distribution in Electrical Capacitance Tomography. IEEE Transactions on Instrumentation and Measurement, 2021, 70, 1-11.	2.4	9
58	2D electrical capacitance tomography with sensors of non-circular cross sections using the factorization method. Measurement Science and Technology, 2011, 22, 114003.	1.4	8
59	Water cut measurement of oil–water flow in vertical well by combining total flow rate and the response of a conductance probe. Measurement Science and Technology, 2015, 26, 095306.	1.4	8
60	A Recursive Demodulator for Real-Time Measurement of Multiple Sinusoids. IEEE Sensors Journal, 2018, 18, 6281-6289.	2.4	8
61	Inverse Radon Method Based on Electrical Field Lines for Dual-Modality Electrical Tomography. IEEE Transactions on Instrumentation and Measurement, 2020, 69, 8250-8260.	2.4	8
62	Particle size influence on effective permittivity of particle–gas mixture with particle clusters. Particuology, 2013, 11, 216-224.	2.0	7
63	Digital micro-mirror device-based detector for particle-sizing instruments via Fraunhofer diffraction. Applied Optics, 2015, 54, 5842.	2.1	7
64	Water holdup measurement of oil–water two-phase flow in a horizontal well using a dual-circle conductance probe array. Measurement Science and Technology, 2016, 27, 115101.	1.4	7
65	Particle sizing from Fraunhofer diffraction pattern using a digital micro-mirror device and a single photodiode. Powder Technology, 2018, 332, 351-358.	2.1	7
66	Retrieval of Phase and Temperature Distributions in Axisymmetric Flames From Phase-Modulated Large Lateral Shearing Interferogram. IEEE Transactions on Instrumentation and Measurement, 2021, 70, 1-12.	2.4	7
67	Sparse Zernike Fitting for Dynamic LAS Tomographic Images of Temperature and Water Vapor Concentration. IEEE Transactions on Instrumentation and Measurement, 2022, 71, 1-14.	2.4	7
68	Manchester code telemetry system for well logging using quasi-parallel inductive-capacitive resonance. Review of Scientific Instruments, 2014, 85, 074704.	0.6	6
69	Effects of water vapor addition on NO reduction of <i>n</i> decane/air flames. Energy Sources, Part A: Recovery, Utilization and Environmental Effects, 2020, 42, 1526-1540.	1.2	6
70	Ultra-Low Sampled and High Precision TDLAS Thermometry Via Artificial Neural Network. IEEE Photonics Journal, 2021, 13, 1-9.	1.0	6
71	?m-resolution thickness distribution measurement of transparent glass films by using a multi-wavelength phase-shift extraction method in the large lateral shearing interferometer. Optics Express, 2019, 27, 2899.	1.7	6
72	The Study of a 2D Model and Image Reconstruction Algorithms Based on EIT System. , 2006, , .		5

#	Article	IF	CITATIONS
73	Electrical resistance tomography(ERT) by using an ECT sensor. , 2010, , .		5
74	An adaptive algorithm for cross-correlation velocity measurement. , 2012, , .		5
75	A chemi-ionization processing approach for characterizing flame flickering behavior. , 2015, , .		5
76	Support-vector-regression-based prediction of water holdup in horizontal oil-water flow by using a bicircular conductance probe array. Flow Measurement and Instrumentation, 2017, 57, 64-72.	1.0	5
77	On-line fuel identification using optical sensing and Support Vector Machines technique. , 2009, , .		4
78	A fast eddy current forward solver for EMT based on finite element method (FEM) and negligibly coupled field approximation. , 2011, , .		4
79	Direct image reconstruction for 3D electrical resistance tomography by using the factorization method. , 2012, , .		4
80	Laser spot center location by using the gradient-based and least square algorithms. , 2013, , .		4
81	Compressive sensing-based wideband capacitance measurement with a fixed sampling rate lower than the highest exciting frequency. Measurement Science and Technology, 2016, 27, 035006.	1.4	4
82	Reconstruction of two-dimensional temperature distribution in swirling flames using TDLAS-based tomography. , 2017, , .		4
83	Dynamic Characterization of Pulse Combustion by Image Series Processing. IEEE Sensors Journal, 2018, 18, 9682-9690.	2.4	4
84	Optimal selection of spectral lines for multispectral absorption tomography. Applied Physics B: Lasers and Optics, 2018, 124, 1.	1.1	4
85	Verification for Electrical Tomography in Flame Monitoring by Ion Probe. , 2019, , .		4
86	A new simplified mechanism for combustion of RP-3/Jet-A kerosene. Energy Sources, Part A: Recovery, Utilization and Environmental Effects, 2020, 42, 676-687.	1.2	4
87	Four-terminal scheme used in a two-terminal EIT system. , 2011, , .		3
88	ℓ <inf>1</inf> Norm based reconstruction algorithm for particle sizing. , 2011, , .		3
89	An alternative digital multiplication demodulation method for electrical capacitance tomography. , 2012, , .		3
90	Direct image reconstruction for ERT by using measurements on partial boundary. , 2013, , .		3

#	Article	IF	CITATIONS
91	Measurement of axisymmetric temperature distributions using single view fan-beam TDLAS tomography. , 2013, , .		3
92	Compressive sensing for particle size retrieval by using a digital micro-mirror device-based detector. Powder Technology, 2016, 304, 27-31.	2.1	3
93	An Iterative Algorithm Based on the Dual Integral Inversion for Particle Sizing. IEEE Transactions on Instrumentation and Measurement, 2018, 67, 1729-1737.	2.4	3
94	Forward solver for deep earth exploration and induction logging using custom built Edgeâ€Element FEM technique. Acta Geologica Sinica, 2019, 93, 302-304.	0.8	3
95	Adaptive Selection of Truncation Radius in Calderon's Method for Direct Image Reconstruction in Electrical Capacitance Tomography. Sensors, 2019, 19, 2014.	2.1	3
96	A Compact Noise-Immune TDLAS Temperature Sensor using Intensity Modulation. , 2020, , .		3
97	Revised Calderon Method of Annular ECT for Imaging Flashback Flame of a Bluff-Body Burner. IEEE Transactions on Instrumentation and Measurement, 2021, 70, 1-10.	2.4	3
98	A direct reconstruction method of electromagnetic tomography(EMT) for high permeability and low conductivity distributions. , 2010, , .		2
99	The experimental research of vortex flowmeter in vertical upward oil-gas-water three-phase flow. , 2010, , .		2
100	Weighting function-based coil size optimization for electromagnetic flowmeter. , 2011, , .		2
101	Direct image reconstruction for electromagnetic tomography(EMT) by using the dbar method. , 2011, , .		2
102	A digital demodulation method for electrical tomography based on sine wave rectification. , 2012, , .		2
103	Image reconstruction algorithm for EMT based on modified Tikhonov regularization method. , 2012, , .		2
104	A digital demodulator based on the recursive Gauss-Newton method for electrical tomography. , 2014, , ,		2
105	A high precision method for mapping phase to amplitude in direct digital synthesis and its hardware implementation. Review of Scientific Instruments, 2014, 85, 114704.	0.6	2
106	Distribution retrieval of temperature from its histograms via the tunable diode laser absorption spectroscopy. , 2017, , .		2
107	Fast wavelength modulated TDLAS imaging system for flame monitoring. , 2019, , .		2

108 Excitation Patterns in 3D Electrical Impedance Tomography for Breast Imaging. , 2019, , .

#	Article	IF	CITATIONS
109	Precise wide-band electrical impedance spectroscopy measurement via an ADC operated below the Nyquist sampling rate. Measurement: Journal of the International Measurement Confederation, 2021, 174, 108995.	2.5	2
110	Random vibration-driven continuous-wave CRDS system for calibration-free gas concentration measurement. Optics Letters, 2020, 45, 746.	1.7	2
111	Temperature imaging of Counterflow Diffusion Flames by using TDLAS Tomography. , 2021, , .		2
112	2D ECT for sensors of non-circular cross sections using the factorization method. , 2010, , .		1
113	A simplified model for non-destructive thickness measurement immune to the lift-off effect. , 2011, , .		1
114	DC bias compensation in digital AC-based capacitance measurement for ECT. , 2011, , .		1
115	FPGA-based implementation of Prony demodulation in the multi-frequency EIT system. , 2011, , .		1
116	Influence of installation angle of electromagnetic flowmeter on measurement accuracy. , 2012, , .		1
117	Simulation on measuring of nonuniform temperature distribution based on line-of-sight TDLAS by using Tikhonov regularization method. , 2012, , .		1
118	Optimization of the Electromagnetic Wave Resistivity tool in Logging While Drilling. , 2013, , .		1
119	Factorization method for electrical resistance tomography with partial boundary measurements. , 2014, , .		1
120	Identification of oil-water flow patterns using conductance probe in vertical well. , 2015, , .		1
121	A linear temperature extraction method from Voigt lineshape profile in laser absorption spectroscopy. , 2020, , .		1
122	A Interferometer modulated TDLAS Temperature Sensor by using Coherent Demodulation. , 2022, , .		1
123	A new strategy for robot path planning based on the finite element method. Proceedings of SPIE, 2008,	0.8	0
124	2D ECT with square sensor using Calderon's method. , 2009, , .		0
125	A new analytical inversion to Fraunhofer diffraction. , 2009, , .		0
126	Direct image reconstruction for electromagnetic tomography by using the factorization method. , 2011, , .		0

#	Article	IF	CITATIONS
127	3D simulation on influence of insulating contents to contactless electromagnetic induction flowmeter. , 2012, , .		0
128	Fan-beam TDLAS tomography for gas concentration distribution with limited data. , 2012, , .		0
129	A high frequency digital induction system for low conductivity object measurements. , 2012, , .		0
130	A direct reconstruction algorithm for recovering the admittivities in 2D electrical tomography. , 2012, , .		0
131	One-dimensional tomography of axisymmetric temperature distribution with limited TDLAS data by using three-point Abel deconvolution. , 2014, , .		0
132	Analysis of the electromagnetic wave resistivity tool in deviated well drilling. , 2014, , .		0
133	A noncontact conductivity detection method based on the principle of electromagnetic induction. , 2015, , .		0
134	Direct methods for image reconstruction in electrical capacitance tomography. , 2015, , 377-399.		0
135	Ghost imaging of binary-valued objects by using a CCD and an equivalent photodiode. , 2015, , .		0
136	Effects of views and spectral lines numbers on hyperspectral temperature distribution tomography. , 2016, , .		0
137	Reconstruction of temperature distribution for swirling flames using one-dimensional TDLAS tomography. , 2016, , .		0
138	Local integrated absorbance tomography based on revised iterative reconstruction-reprojection algorithm. , 2017, , .		0
139	Recent development of electromagnetic wave resistivity tools for loggingâ€whileâ€drilling. Acta Geologica Sinica, 2019, 93, 291-291.	0.8	0
140	A survey of underground detection methods with a new proposal for urban underground detection. Acta Geologica Sinica, 2019, 93, 322-324.	0.8	0
141	A robust Doppler shift-based velocimetry via using tuable diode laser absorption spectroscopy. , 2019, , ·		0
142	A Multi-frequency WMS Method for Tunable Diode Laser Absorption Spectroscopy Tomography. , 2019, , ,		0
143	Special Section on Imaging Systems and Techniques 2017. Measurement Science and Technology, 2019, 30, 020103.	1.4	0
144	A flexibly reconfigurable data acquisition system for tunable diode laser absorption spectroscopy. , 2020, , .		0

#	Article	IF	CITATIONS
145	Dynamic flashback induced by sound wave in a premixed bluff-body stabilized flame. IOP Conference Series: Earth and Environmental Science, 2020, 546, 042019.	0.2	0
146	Absolute Wavenumber Determination for Distributed Feedback Laser from Absorption Spectral Profiles. , 2021, , .		0
147	Dynamic measurement of thickness distribution in a soap film by using a phase-modulated large lateral shearing interferometer. , 2021, , .		0
148	The Study of a 2D Model and Image Reconstruction Algorithms Based on EIT System. Conference Record - IEEE Instrumentation and Measurement Technology Conference, 2006, , .	0.0	0
149	RBF-based reconstruction method for tomographic imaging of temperature and water vapor concentration in flames. , 2021, , .		0
150	Direct image reconstruction in electrical tomography and its applications. , 2022, , 389-425.		0
151	Temperature Telemetry with Synchronous Distance Detection System based on CM-TDLAS. , 2022, , .		0